"Prediction of Boundary Layer Transition on Transonic Swept Wings"

M. Mirshams

Bombardier Aeronautical Chair Group
École Polytechnique de Montréal
P.O Box 6079, Station A
Montréal, H3C 3A7, Canada.

1. INTRODUCTION

Since the last successive oil crises, all civil aircraft manufacturers have made great efforts to reduce overall drag on aircraft. The long term objective of this effort is to reduce the specific fuel consumption and the operating costs. An important reduction of the skin friction, which contributes as much as 50% of the total drag on commercial aircraft can be achieved by maintaining a laminar boundary layer over the longest extent possible of the wetted aerodynamic surfaces.

More than a century of research in fluid mechanics has provided only a few guidelines for design engineers to predict the point of laminar/turbulent transition in a boundary layer. The most promising approach for studying boundary layer transition phenomenon is the Direct Numerical Simulation (DNS) based on Navier-Stokes formulation. Unfortunately, the computational capacity and time associated with this method are enormous and the costs incurred are prohibitive for most industrial design applications.

A more appealing strategy is to obtain a cheaper but adequate approximation on the location of transition from predictions based on Linear Stability Theory [1]. This theory investigates the behaviour of the instability waves that propagate inside the boundary layer at a fraction of the free-stream velocity, and may grow or damp with time (temporal stability theory) or space (spatial stability theory).

2. LINEAR STABILITY THEORY

General Formulation

The local cartesian coordinate system defined in Fig. 1 is used to derive the linear stability equations. The instantaneous flow variables (i.e the velocity components U,V,W in the mainstream (x), normal (y) and spanwise (z) directions, the pressure P and the temperature T) are decomposed into a mean and a perturbation field, under the assumption that the flow is locally parallel:

$$
\begin{Bmatrix} U(x,y,z,t) \\ V(x,y,z,t) \\ W(x,y,z,t) \\ P(x,y,z,t) \\ T(x,y,z,t) \end{Bmatrix} = \begin{Bmatrix} U_o(y) \\ 0 \\ W_0(y) \\ P_0 \\ T_0(y) \end{Bmatrix} + \begin{Bmatrix} \tilde{u}(y) \\ \tilde{v}(y) \\ \tilde{w}(y) \\ \tilde{p}(y) \\ \tilde{\tau}(y) \end{Bmatrix} e^{i(\alpha x + \beta z - \omega t)} \quad (1)
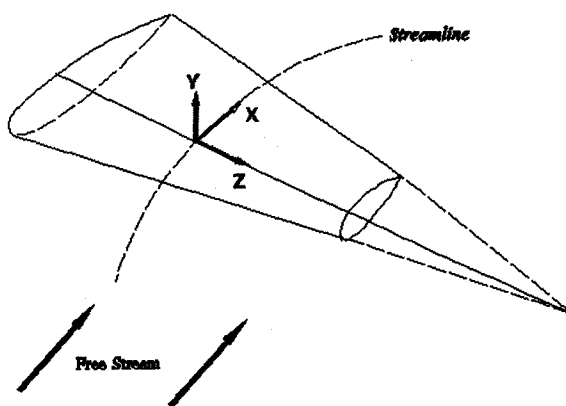$$

Figure 1 - Local Coordinate System Used

The Locally parallel flow assumption implies that the mean velocity components U_0 and W_0 depend on y only. It follows from the continuity equation that the mean normal velocity field, V_0, is identically zero over the entire domain, which in turn implies that the pressure gradient in the boundary layer is zero ($\frac{\partial P_0}{\partial y} = 0$). Thus, the validity of this model is limited to areas where curvature effects can be neglected and where the growth rates of δ_e and δ_1 are small. For moderate to large Reynolds numbers, R_e, the error associated with this approximation can be considered small so that solutions of the linear stability equations are expected to yield adequate estimations of the transition point over airfoils.

$\alpha = \alpha_r + i\,\alpha_i$ and $\beta = \beta_r + i\,\beta_i$ are the chordwise and the spanwise complex wavenumbers, which give the wave spacing. The real part of α yields the chordwise wavenumber and the imaginary part yields the chordwise spatial growth rates. The real part of β gives the spanwise wavenumber and the imaginary part represents the spanwise spatial amplification factor. $\omega = \omega_r + i\,\omega_i$ is the wave complex frequency. The real part of ω is the real frequency and the imaginary part gives the temporal amplification factor.

The system of equations to be solved for this analysis are obtained by substituting the definitions of Eq.(1) in the three momentum and the energy transport equations. The non−linear and the second−order terms are then neglected to yield a second−order system of five linearized equations. For the purpose of this analysis, only the homogeneous solution is of interest. Hence, the particular solution, which represents the average velocity and temperature fields and is assumed known *a priori*, can be removed simply by subtracting the averaged Navier−Stokes and energy equations from the linearized system. The resulting system of equations can thus be written in compact matrix form as:

$$([A]D^2 + [B]D + [C])\,\vec{\Phi} = 0 \qquad (2)$$

where D denotes the operator $\frac{d}{dy}$; [A], [B] and [C] are 5×5 matrices dependent upon the boundary layer components and disturbance characteristics; and $\vec{\Phi}$ is the five−element perturbation vector, defined as:

$$\vec{\Phi} = \begin{Bmatrix} \phi_1 \\ \phi_2 \\ \phi_3 \\ \phi_4 \\ \phi_5 \end{Bmatrix} = \begin{Bmatrix} \alpha\,\tilde{u} + \beta\,\tilde{w} \\ \tilde{v} \\ \tilde{p} \\ \tilde{\tau} \\ \alpha\,\tilde{w} - \beta\,\tilde{u} \end{Bmatrix} \qquad (3)$$

It is worth noticing at this point that to obtain this form of the perturbation vector, the Stuart transformation [2] *is applied*. In three−dimensional incompressible flows, this transformation allows a two−dimensional stability analysis. Moreover, it should be noted that the system is represented in nondimensional form. The boundary conditions at the surface of the airfoil ($y = 0$) and in the far stream ($y \to \infty$) are *homogeneous*, i.e. the disturbances must vanish at the wall and in the free stream, except for the pressure fluctuations which have a non−zero amplitude at the wall. However, since a staggered grid is used, the need for a boundary condition for the pressure field, ϕ_3 , is obviated:

$$y = 0 \quad \Rightarrow \quad \phi_i = 0$$
$$y \to \infty \quad \Rightarrow \quad \phi_i \to 0 \qquad i \in \{\,1,2,4,5\,\} \quad (4)$$

The question of stability of the boundary layer is whether the solutions of Eq. (2) along with boundary conditions (4) contain disturbances that grow or decay in time or space. At a given position on the wing, where the boundary layer and the Reynolds number are specified, non−trivial solutions exist only for certain combinations of the parameters α, β and ω . The analysis of this system of equations constitutes an *eigenvalue problem* for α, β and ω which are generally

complex. A solution can only be found for one of the parameters so that values for the other two must be determined independently. It is common practice to make some basic assumptions as to the nature of these parameters which lead to two distinct theories:

−Imposing that α and β be real places the problem in the context of the *temporal stability theory* in which disturbances grow or dacay with time only. Thus, the temporal amplification rate of a disturbance is given by the imaginary part of the complex frequency, ω_i. The disturbance is amplified when $\omega_i > 0$.

−For the *spatial stability theory* in which disturbances grow or dacay in space only, ω is assumed real and the imaginary parts of the wavenumbers, α_i, β_i yield the spatial growth rate in the streamwise and spanwise directions. The disturbance is amplified in both directions when $\alpha_i, \beta_i < 0$.

Although the two theories should be equivalent, they deliver complementary information. The spatial theory allows a direct estimation of the spatial growth rate necessary to calculate the N−factors and thus the location of transition. Conversely, the temporal theory supplies frequency information directly but the spatial growth rate is obtained only indirectly.

Discretization

The mathematical model described in the previous section is, in general, not amenable to an analytical solution. Consequently, the solution procedure proposed here is based on numerical techniques. It is convenient to map the physical domain $0 \leq y \leq \delta_e$ onto $0 \leq \eta \leq K$ as presented in Fig. 2, viz:

$$\eta = K \frac{g\,y}{L + y}, \quad g = 1 + \frac{L}{\delta_e} \qquad (5)$$

where L is chosen to be approximately twice the distance from the wall to the point where $U_0 = \frac{1}{2} U_e$ (*critical layer*) and K is an arbitrary, positive integer representing the number of grid points for the stability analysis. This transformation offers two distinct advantages. First, an equidistant grid in the mapped region can be used, which allows a fine resolution in the *critical layer* of the velocity profile. Second, the approximations for the first and second derivatives of the perturbation quantities using finite differences are second order accurate.
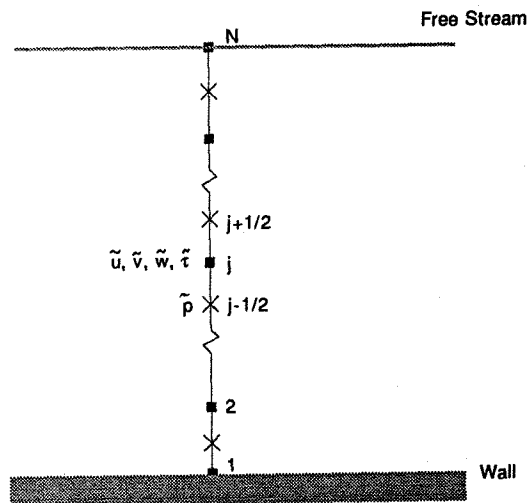
Figure 2 − Staggered Finite−Difference Grid Used

The differential equation (2) is then discretized using K grid points to yield:

$$(\omega\, [M_1] + \alpha\, [M_2] + \alpha^2\, [M_3] + \beta\, [M_4] + \beta^2\, [M_5] + [M_6])\, \{\vec{\Phi}\} = 0 \qquad (6)$$

where M_i are $5K \times 5K$ matrices and $\{\vec{\Phi}\}$ is a 5K vector corresponding to the 5 discretized

eigenfunctions at each grid point. The resulting system of equations is not mathematically closed since there are more unknown parameters than equations. It is thus customary and necessary to make some basic assumptions about the nature of α, β and ω.

Temporal Stability Theory

In the temporal stability theory, α and β are assumed to be real. For given values of α and β, the system of equation is amenable to a *linear eigenvalue problem in L*:

$$[P_s] \{\vec{\Phi}\} = \omega [M_1] \{\vec{\Phi}\} \qquad (7)$$

Because the eigenvalue appears linearly in the temporal form of stability equations, the first stability calculations concentrated on this theory.

A computer code based on *temporal* stability theory was developed by the Bombardier Aeronautical Chair Group of Ecole Polytechnique [3]. In this computer code, the global calculations are based on the QZ algorithm of the IMSL library. If the eigenvalue problem is descretized using K grid points, the complete discrete spectrum consists of 5K eigenvalues. The local method chosen is the *inverse Rayleigh iteration* procedure.

Spatial Stability Theory

In the spatial stability theory, ω is assumed to be real and given, α and β are complex. Assuming β known the resulting system of equations can thus be expressed as a *nonlinear eigenvalue problem in* A:

$$[P_s] \{\vec{\Phi}\} = (\alpha [M_2] + \alpha^2 [M_3]) \{\vec{\Phi}\} \qquad (8)$$

Spatial theory corresponds more closely to certain physical situations such as boundary layers. Recently, the author has developed a *spatial* stability analyzer [5] which is the main

subject of this paper. In the spatial stability theory, the resulting eigenvalue problem is *nonlinear in* α. Such a nonlinear discrete eigenvalue problem can be solved using several methods. In this paper, the approach used to solve the spatial eigenvalue problem is the linearized problem given by:

$$[P_s] \{\vec{\Phi}\} = \alpha ([M_2] + \alpha_{guess}[M_3]) \{\vec{\Phi}\} \qquad (9)$$

where α_{guess} represents the value of the initial *guess* for the eigenvalue of interest.

The imaginary part of the guess could be obtained by using the temporal analysis and Gaster's relation [4]:

$$(\alpha_i)_{guess} = \frac{-\omega_i}{\|\vec{V}_{gr}\|} \qquad (10)$$

General Eigenvalue Problem

The system, rewritten in the form of Eq.(6), is expressed to suit the eigenvalue problem solution for:

$$\{ [E] - \xi [F] \} \{\vec{\Phi}\} = 0 \qquad (11)$$

where ξ is the eigenvalue corresponding either to ω for the temporal theory or α in the linearized spatial theory. Using the staggered grid detailed earlier at any *station* on the wing, the discretized equations along with the boundary conditions are formulated as a *matrix eigenvalue problem*. This is a large block−tridiagonalsystem of equations of order $5K$ with 5×5 blocks.

This eigenvalue system can be solved using classical numerical algorithms. These methods can be divided into two categories, namely *global methods* and *local methods*. Global methods are used to obtain the complete eigenvalue spectrum. They are quite expensive in terms of computational

1484

resources but they do not need any initial guess of the eigenvalue. On the other hand, when one is interested in a particular eigenvalue, local methods are more efficient. However, such procedures need an initial guess of the eigenvalue of interest.

In this project, the solution is first determined on a coarse grid using a *global method* to yield the entire eigenvalue spectrum. For this purpose, a standard IMSL—packageroutine based on the QZ algorithm is used. The system to resolve is naturally ill—conditionedso that a *global method* is inefficient and can be economically prohibitive to use when a very accurate eigenvalue is sought on a fine grid. Thus, the *global method* is only used together with a coarse grid to obtain an initial estimate (*guess*) for the eigenvalues. Since only the amplified waves are of interest, refined estimates of the eigenvalues are only calculated for cases where the imaginary part of the eigenvalue solution satisfy $\omega_i > 0$, for the temporal theory, or $\alpha_i < 0$ for the spatial theory. These values are subsequently refined using a *local method* based on the inverse Rayleigh iteration procedure. This method is advantageous since it has a cubic rate of convergence and involves only the calculation of the relevant eigenmodes.

Group Velocity Concept

In a non—dispersive media (such as for the propagation of electromagnetic waves in outer space) all frequencies propagate with the same speed called the *phase velocity*. A boundary layer, however, is a dispersive media for the propagation of instability waves. In other words, different waves with different frequencies would propagate with different phase velocities. In such a media, the energy density or amplitude propagates with the *group velocity*. Group velocity represents the velocity of a group of waves at one time, that will be dispersed from each other at some later time. The group velocity of a specified frequency is a property of that individual wave, and to follow the

behavior of a particular instability one should use the group velocity of that particular frequency (Fig. 3). For an observer moving at the group velocity of a given frequency, the wave in the moving frame of reference will appear to undergo temporal amplification, while in the frame at rest it undergoes spatial amplification. Furthermore, because of damping and amplification, instability waves constitute a non—conservativesystem, and the group velocity is, in general, composed of a real and an imaginary part. The group velocity is expressed as :

$$\vec{V}_g = \left(\frac{\partial \omega}{\partial \alpha} , \frac{\partial \omega}{\partial \beta} \right) \qquad (12)$$
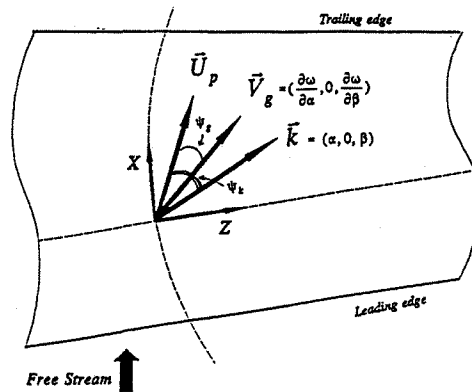

Figure 3 - 3D Group Velocity and Wavenumber Vector

Transition Prediction Using e^N Method

The linear stability theory allows the calculation of the amplification factor of a laminar flow field. However, the main objective of this project is transition prediction. Therefore, a relation between the amplification factor and the transition location is needed. The so—called e^N *method* provides this relation. In this method, the N—factor is calculated by integrating the spatial amplification

factor (γ_i) along the path of propagation (s) which is parallel to the real part of the group velocity, $\vec{V}_{gr}$:

$$N(s) = \int_{s_0}^{s} - \gamma_i \, ds \qquad (13)$$

where s is the relative chord position and s_0 is the point where $(\gamma_i = 0)$. The transition is assumed to occur when the N−factor reaches the critical value of $N_{cr} \cong 9$. The spatial amplification factor (γ_i) is given by the effective growth rate of a perturbation along its path of propagation, and is obtained according to:

$$\gamma_i \, ds = \alpha_i \, dx + \beta_i \, dz$$

where ds is parallel to the real part of the group velocity, $\vec{V}_{gr}$ at all points.

Assuming β_r known and that the wave can only be amplified in the x direction (i.e β_i set equal to zero), the spatial amplification factor in the streamwise direction, α_i, is a direct result of the *nonlinear eigenvalue problem* of the spatial stability theory. The spatial amplification factor in the direction of the real part of the group velocity is given by:

$$\gamma_i = \alpha_i \frac{Re\left\{\dfrac{\partial \omega}{\partial \alpha}\right\}}{\| \vec{V}_{gr} \|} \qquad (14)$$

However, in the temporal stability theory, the spatial amplification factor in the direction of the real part of the group velocity is obtained from the temporal amplification factor through the application of *Gaster's relation* [4]:

$$\gamma_i = - \frac{\omega_i}{\| \vec{V}_{gr} \|} \qquad (15)$$

which involves the knowledge of the group velocity. The range of validity of Gaster's relation

remains largely uninvestigated. Therefore, the spatial stability theory seems promising since Gaster's relation is not needed. However, the spatial formulation yields a nonlinear eigenvalue problem in α which is a much more involved problem than the linear eigenvalue problem in ω of the temporal formulation.

3. RESULTS AND DISCUSSION

The results of three validation tests for different airfoils will be presented in this section to assess the ability of the proposed boundary layer stability analyzer to predict the location of transition. The rather limited availability of experimental transition data basically determined the selection of suitable candidate airfoils for the validation tests. These cases were selected from the literature where the measured surface pressure distributions and an observed estimate to the location of transition were available.

The boundary layer solution is calculated by the commercially available Cebeci−Kaups code [6], using as input the airfoil geometry, pressure coefficient distribution and suction distribution. This code has proven very effective in transonic applications with a conical pressure field.

All stability calculations are performed on the upper surface of the airfoil, using K=21 grid points for the stability analysis.

1486

NAE-76-060 13:1 Airfoil Test

The NAE$-$76$-$060 profile is a thick supercritical airfoil with low drag, and was tested at the National Research Council of Canada wind tunnel in Ottawa [8]. This test was designed to study the compressible (transonic regime) and three$-$dimensional effects. This profile exhibits the 'top$-$hat' pressure distribution typical of NLF$-$airfoils operating in the transonic regime (Fig. 4). It should be noted that the 'dip' in the pressure distribution illustrates the presence of a shock wave. The presence of the shock wave is a determining factor for the on$-$setof transition for this profile. Typically, transition occurs shortly upstream of the shock or it is the shock wave itself which directly triggers transition.
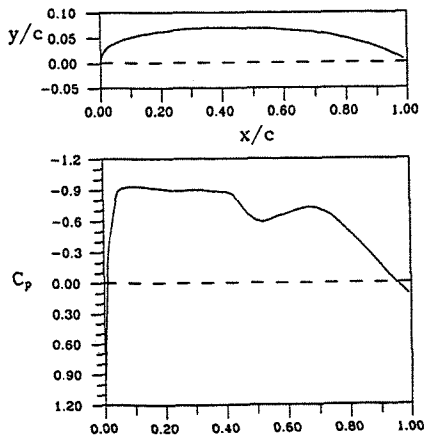

Figure 4$-$ Geometry and Pressure Distribution for the NAE$-$76$-$06013:1 airfoil

The N$-$factor data obtained from both temporal and spatial stability theories for the most unstable frequency are shown in Fig. 5. The predicted location of transition by both theories occurs very close to that observed experimentally. In fact, the calculations indicate that this profile design is extremely effective at suppressing the inception of instabilities. Namely, the N$-$factorcurves grow up to $\frac{x}{c} \approx 0.35$ and then increase very rapidly up to

the point of transition at $\frac{x}{c} \approx 0.45$ due to the disturbance of the boundary layer caused by the presence of the shock wave, through the adverse pressure gradient.

Such NLF profiles are designed to produce favorable chordwise pressure gradients. Although this favorable pressure gradient could control the growth of TS$-$waves, on a swept wing it can amplify crossflow growth. The results shown in Fig. 6 are representative of both kinds of instability for this profile. For the region close to the leading edge ($\frac{x}{c} < 0.17$), the wavevector associated with the disturbances is almost normal to the main flow direction ($90° < \psi_k < 100°$), where these instabilities are propagating normal to the flow. There is then an abrupt change in wavevector orientation as the crossflow mechanism becomes less significant. This typical 'jump' is characterized by the fact that the wavenumber vector aligns with the group velocity and the main flow direction ($\psi_k, \psi_g \to 0$). This behavior is typical of airfoils with two distinct regions of instability, crossflow at the leading edge and streamwise downstream.
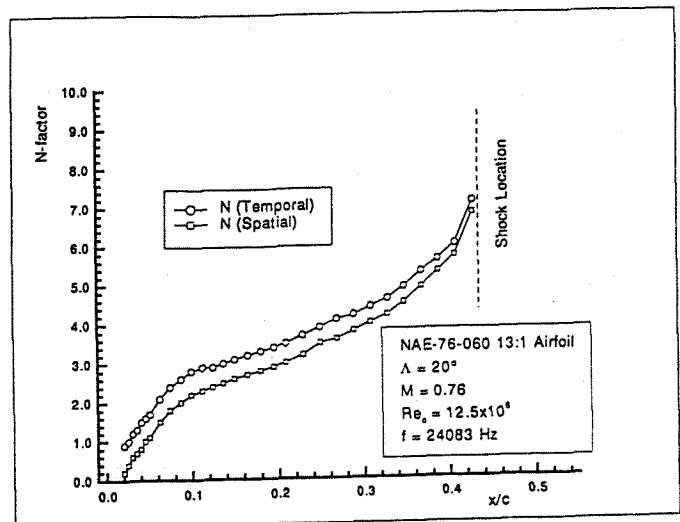
Figure 5 $-$ N$-$factor Calculation for the NAE$-$76$-$060 13:1 Airfoil
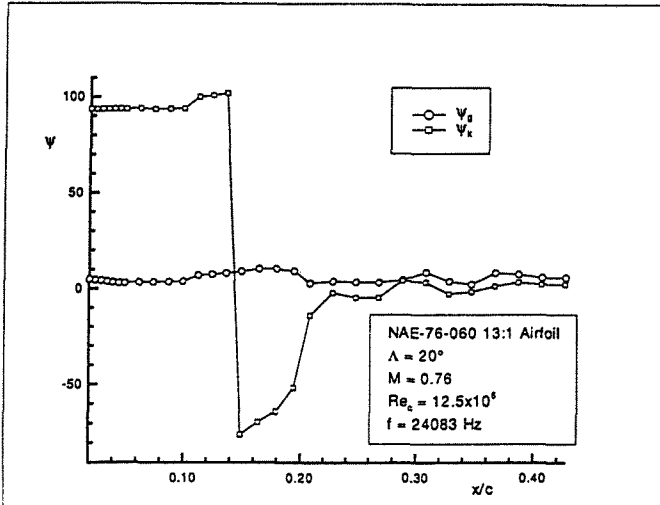
1487

Figure 6 – Wave Orientation for the NAE–76–060 13:1 Airfoil

NLF(2)-0415 16:1 Airfoil Test

The NLF(2)−0415 airfoil test is a low Mach number, high Reynolds number case. These conditions are not ideal for testing the code because the program was designed for compressible flows. It is felt, however, that the code should still be applicable to these cases.

The pressure distribution for this airfoil is not typical of NLF airfoils in that it does not display the characteristic plateau, or 'top−hat' form (Fig. 7). The NLF(2)−0415 airfoil possesses a favorable pressure gradient up to approximately 60% relative chord length.

Whereas the experiments [9] suggest that for this airfoil transition occurs at approximately $0.50 \leq \frac{x}{c} \leq 0.55$, the N−factor calculations based on a critical N−factor of 9 predict the location to be at $\frac{x}{c} \approx 0.35$. This discrepancy can be explained. Since the wind tunnel used in the experimental study is described as being of very low intensity level, one may recall that for free flight conditions a critical N−factor of 12 is often suggested.
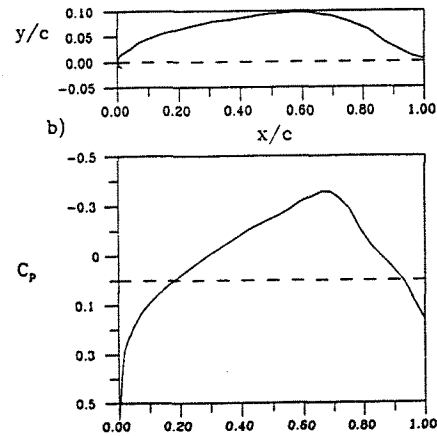

Figure 7 – Geometry and Pressure Distribution for the NLF(2)−0415 16:1 Airfoil
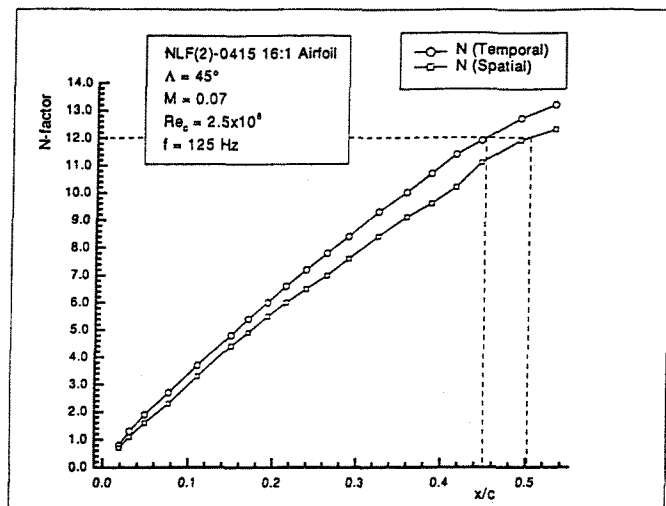

Figure 8 – N−factor Calculation for the NLF(2)−0415 16:1 Airfoil

Using this criterion places transition now at $\frac{x}{c} \approx 0.50$. Hence, the results of this test imply that the $N_{cr} \approx 9$ criterion is not universally applicable. It is strongly recommended that caution be exercised in interpreting results for extremely quiet wind tunnels or free flight tests.

As a guide line, the empirical relationship for selecting the *critical N-factor*, proposed in an earlier investigation by Mack [10], viz:

$$N_{cr} = -8.43 - 2.4 \ln T_u \qquad (16)$$

where T_u is the turbulence intensity, is put forth to obtain an estimate for an adequate critical N−factor.This is called the *modified e^N method*. Unfortunately, T_u is often not available. Under these circumstances, critical values of the N−factor between 9 and 12 should be considered for cases where the free stream turbulence intensity is expected to be particularly low.

Furthermore, comparing N−factors obtained by both theories (temporal and spatial) it can be noticed that the transition location based on the spatial theory is closer to that observed experimentally. It is also interesting to mention that the most unstable frequencies predicted are between 100 Hz and 200 Hz, which correlates well with the experimental findings.

YEBZ-244 Sucked Airfoil Test

As a result of three−dimensionaleffects, laminar flow swept wings appear to be more difficult to maintain than on unswept wings. Suction as a mean of Laminar Flow Control (LFC) is then expected to reduce both crossflow and streamwise instabilities over the wing. Since the aim should be to apply just enough suction so that the N−factors do not grow beyond a value of 9, the first step to estimate an optimum suction distribution is to accurately calculate the stability characteristics of the boundary layer.

Suction has several effects on the boundary layer. First, it causes the inflection point of the crossflow profile to move closer to the wall, where the increased viscosity acts to stabilize the crossflow instability. Secondly, suction thins the boundary layer and thereby lowers the effective Reynolds number. Suction also results in a shift of the most

amplified wave to a lower frequency. All these effects are known to have stabilizing influence on the boundary layer stability. The YEBZ−244airfoil is an example of how suction could lead, at least theoretically, to a fully laminar wing. The geometry, pressure and suction distributions for this case are shown in Fig. 9.
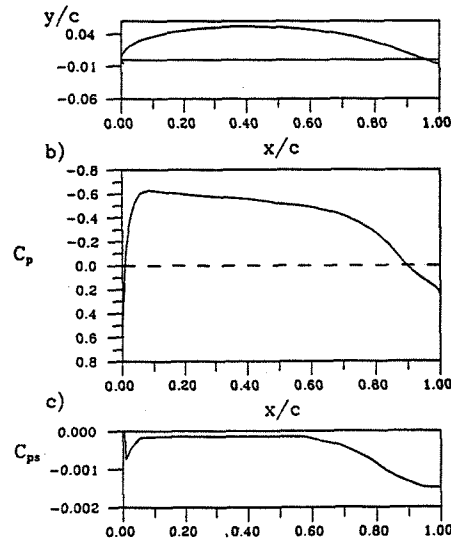
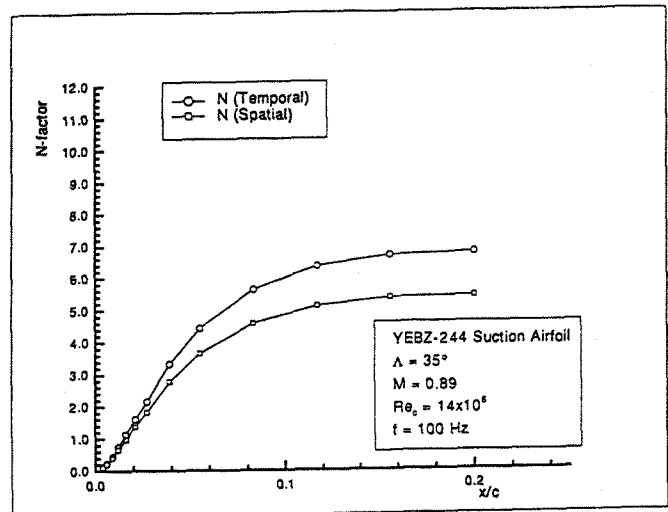Figure 9 − Geometry, Pressure and Suction Distributions for the YEBZ−244 airfoil
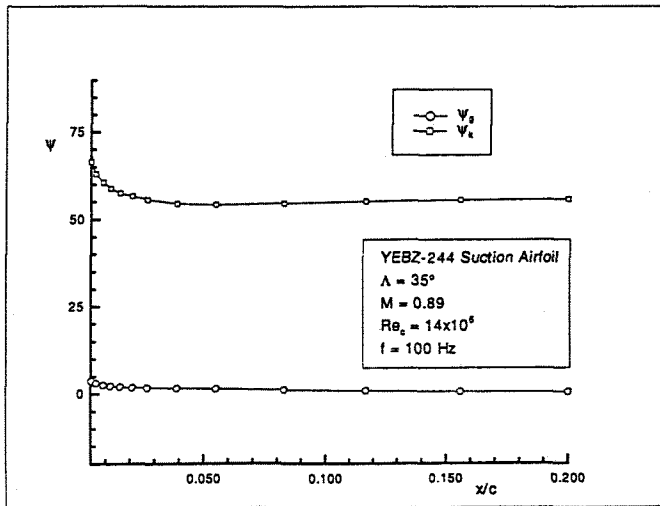
Figure 10 − N−factorCalculation for the YEBZ−244 Sucked Airfoil

Figure 11 —Wave Orientation for the YEBZ—244 Sucked Airfoil

The largest N—factors computed are found for a frequency around f=100 Hz. It can be seen in Fig. 10 that the amplitude of oscillations may become important but suction effectively suppresses transition. Furthermore, it is noticed that the largest amplification is found to be for oblique waves of about $\psi_k \simeq 50°$ (Fig. 11). In fact, the orientation angle of the most amplified wave seems to be stabilized as a result of suction application.

Although the estimated suction distribution is adequate to maintain laminar flow, it is not necessarily the optimum distribution. The boundary layer should not be oversucked, since that has several adverse effects, e.g., larger perturbations caused by the suction holes, increased skin friction and increased weight of the suction system. An iterative application of the boundary layer stability analyzer could then help to achieve the optimum suction distribution.

4.   CONCLUSION

The comparison of predicted and experimental locations of transition for several swept wings under different conditions shows that spatial linear stability theory provides an estimate which generally agrees within 5% of the relative chord $(\frac{x}{c})$. These predictions are consistently conservative, i.e. the location is under predicted, which is desirable from the point of view of design. The results for three airfoils are presented in this paper. It is clear that further work is needed to improve the tools developed up to now. These tools have to be validated with respect to transition prediction and experimental verification. Therefore, more reliable transition data including flight experiments and transonic wind tunnel tests with low turbulence intensity and highly flow quality are indispensable.

5.   REFERENCES

[1]   Lees, L., Lin, C.C., "*Investigation of the Stability of the Laminar Boundary Layer in a Compressible Flow*", NACA Technical Note, No. 1115, 1946.

[2]   Gregory, N., Stuart, J.T., Walker, W.S "*On the Stability of Three-Dimensional Boundary Layers with Application to the Flow due to Rotation Disk*", Philosophical Transactions of the Royal Society of London, Vol. A248, pp. 155—199, 1955.

[4]   Gaster, M., "*A Note on the Relation Between Temporally Increasing and Spatially Increasing Disturbances in Hydrodynamic Stability*", J. of Fluid Mechanics, Vol. 14, pp. 222—224, 1962.

[3] Martinuzzi, R., Lamarre, F., Paraschivoiu, I., *"Natural Laminar Flow Airfoils for Swept Wings in the Transonic Regime"*, Final Report to Canadair Aerospace Group, Ecole Polytechnique de Montréal, September 1992.

[5] Mirshams, M., Masson, C., Paraschivoiu, I. *"Further Development in the Implementation of the Spatial Stability Theory"*, Progress Report to Canadair Aerospace Group, Ecole Polytechnique de Montréal, January 1994.

[6] Kaups, K., Cebeci, T., *"Compressible Laminar Boundary Layers with Suction on Swept and Tapered Wings"*, AIAA Journal of Aircraft, Vol. 14, pp. 661–667, 1977.

[7] Khorrami, M.R., and Malik, M.R., *"Efficient Computation of Spatial Eigenvalues for Hydrodynamic Stability Analysis"*, J. of Computational Physics No 104, p. 267, 1993.

[8] Khalid, M., Jones, D.J.*"A Summary of Transonic Natural Laminar Flow Airfoil Development at NAE"*, Aeronautical Note, NAE–AN–65,NRC Report 31608, May 1990.

[9] Agarwal, N.K., Maddalon, D.V., Mangalam, S.M. and Collier, F.S.,*"Crossflow Vortex and Transition Measurements by Use of Multielement Hot Films"* AIAA Journal, Vol.30, No. 9, Sept. 1992, pp. 2212–18.

[10] Mack, L.M., 'Transition Prediction and Linear Stability Theory', AGARD Conference Proceedings No. 227, pp.1–1:1–22,1977.